High-resolution inner-valence uv photoelectron spectra of the O_2 molecule and configuration-interaction calculations of $^2\Pi_u$ states between 20 and 26 eV

P. Baltzer, B. Wannberg, L. Karlsson, and M. Carlsson Göthe
Uppsala University, Department of Physics, Box 530, S-751 21 Uppsala, Sweden

M. Larsson
Department of Physics I, Royal Institute of Technology, S-100 44 Stockholm, Sweden
(Received 16 October 1991)

High-resolution He I and He II excited inner-valence photoelectron spectra of the oxygen molecule have been recorded between 20 and 26 eV. In this range three photoelectron bands are clearly observed that are associated with transitions to the $B\,^2\Sigma_g^-$, $^2\Pi_u$, and $c\,^4\Sigma_u^-$ cationic states. Vibrational structure is observed in all photoelectron bands, and the vibrational constants have been determined. The rotational profile of the vibrational lines is resolved for the B state, and an analysis is made in terms of transitions involving $\Delta N=0$ and ± 2. In addition to the three strong bands, a fourth, weak vibrational progression has been observed in the range of the $B\,^2\Sigma_g^-$ state. The state of $^2\Pi_u$ symmetry observed around 24 eV shows a long vibrational progression with spacings that decrease successively towards higher electron binding energies. The progression converges at 23.83 eV, slightly below the position where the band has the highest intensity. This $^2\Pi_u$ state is thus shown to be bound with a dissociation energy D_0 of 2.5 eV. The assignments are confirmed by *ab initio* calculations, which also provide a vibrational analysis and potential curves that agree very well with the experimental results. These calculations show that the potential curves follow the electron configurations rather than the adiabatic curves in the inner-valence region.

PACS number(s): 33.60.Cv, 31.20.Tz, 33.70.Ca, 33.70.Jg

I. INTRODUCTION

The inner-valence region in the photoelectron spectrum of the oxygen molecule has been the subject of several earlier studies. uv photoelectron spectra were obtained by Edqvist *et al.* [1] Gardner and Samson [2] using He II radiation and by Jonathan *et al.* [3] using both He I and He II radiation as well as a discharge system to study the ionization from excited molecules. In the latter study correlation states in the inner-valence region could be reached in transitions from electronically excited initial states. Also van Lonkhuyzen and de Lange [4] used a microwave discharge to study transitions from the $O_2(^1\Delta_g)$ state but limited the investigation to transitions below 20 eV.

In the range between 20 and 30 eV four comparatively strong photoelectron bands have been observed. The first band, associated with transitions to the $B\,^2\Sigma_g^-$ state, shows an extensive vibrational progression in the range above 20 eV. The second band centered at 24 eV is very broad, on the order of 3 eV, and has in previous studies been considered to be essentially structureless. It corresponds to a state of $^2\Pi_u$ symmetry associated with the third state arising from the $1\pi_u^3 1\pi_g^2$ final-state configuration. We denote this state $3\,^2\Pi_u$ in this report. The third band, which is found in the same energy region, is narrow, consisting essentially of two intense vibrational lines corresponding to the $v=0$ and 1 components of the final state and an additional broad structure reflecting a higher vibrational state. A fourth band has been observed at about 27.3 eV.

In the present investigation we have obtained He I and He II excited photoelectron spectra of the bands present in the energy range between 20 and 30 eV. The study has been carried out using an improved uv source with very good characteristics, which has allowed recordings with both high resolution and intensity. Some of the recordings were carried out with monochromatic He IIα radiation using a new monochromator [5] for the resonance radiation from the uv source. The high-quality spectra obtained provide information useful for the description of the singly ionized states.

Potential curves of the ionic states of $^2\Pi_u$ symmetry occurring in the energy interval considered in the present study have been calculated using the complete active-space (CAS) self-consistent-field (SCF) and contracted configuration-interaction (CI) methods. From these results also vibrational energies and Franck-Condon factors have been derived theoretically. Of special interest is the $3\,^2\Pi_u$ state because its properties have not been well known. In previous theoretical studies [6–8] this state has been found to be bound but to have a rather shallow potential minimum due to interaction with repulsive many-electron states of the same symmetry. The value obtained for the dissociation energy D_e was 0.78 eV in Ref. [6] and 1.06 eV in Ref. [8] and the dissociation limit was in all cases found to be 22.06 eV. For these potential curves the Franck-Condon region for transitions from the neutral ground state falls above the dissociation limit, which implies that no vibrational structure should be observed in the photoelectron spectrum. This conclusion agrees with earlier experimental results, which have indi-

cated that the photoelectron band is structureless. However, in the present study carried out at higher resolution than previously, an extensive vibrational progression is observed which converges towards a higher dissociation limit than 22.06 eV above the neutral ground state. It is suggested from this observation and the calculations that the potential curve dominated by the single hole electron configuration ($1\pi_u^3 1\pi_g^2$), rather than the adiabatic potential curve, describes the vibrational structure of the $3\,^2\Pi_u$ state.

Calculations have also been performed for the second state of $^2\Pi_u$ symmetry arising from the $1\pi_u^3 1\pi_g^2$ final-state configuration. This state, which we refer to as $2\,^2\Pi_u$, is located at about 20 eV and is predicted to have a very low but nonzero photoionization cross section [9]. The results obtained are compared to weak lines in the experimental spectrum which seem to form a vibrational progression.

II. EXPERIMENTAL DETAILS

The measurements were performed by means of an uv-photoelectron spectrometer that has been described in some detail previously [10]. Briefly it is based on an electrostatic hemispherical analyzer with a mean radius of 144 mm and a microchannel plate detector system. An electron lens focuses the photoelectrons onto the entrance slit of the analyzer. The target gas molecules are let into a gas cell where the photoionization takes place. Target gas pressures on the order of 10 mtorr were used in the present investigation. By a recent redesign of the gas cell we have managed to considerably reduce the probability for the processes that contribute to the background in photoelectron spectra [11]. Thus the spectra obtained in the present study are essentially background-free. Other improvements have reduced the leakage of He gas into the gas cell, which inevitably leads to the presence of a helium line in the spectra at 24.587 eV.

The helium radiation employed for the photoionization was produced in a vacuum ultraviolet (vuv) source based on a microwave driven discharge [12,13]. The discharge takes place at a pressure of about 50 mtorr in a very small volume between the pole pieces of a strong magnet which provides a field with the shape of a magnetic bottle fulfilling the electron cyclotron resonance (ECR) condition in the center. This source gives a very high He IIα intensity that makes detailed studies of the inner-valence region feasible. Furthermore, the linewidth of this radiation is very small (on the order of 1 meV). This uv source is now commercially available.

The best resolved spectra presented in this paper were obtained using a pair of correction electrodes in the gas cell developed for these experiments. These electrodes were used to compensate for the potential gradient along the ionizing radiation beam as described in Ref. [11]. This device enables the persistent acquisition of spectra with an instrument contribution to the linewidth of less than 4 meV even at rather high gas-cell pressure levels. All spectra presented in the various figures are shown as originally obtained from the spectrometer. Thus no deconvolution or background subtraction has been made.

The sample gas was obtained commercially with a purity of better than 99.999%. As energy reference for the determination of binding energies the $B\,^2\Sigma_g^-(v=0)$ transition was used. This line has been found to have an energy of 20.296 eV [1] and the linearity of the energy scale is better than ± 2 meV over the entire energy region.

III. COMPUTATIONAL METHODS

The oxygen one-particle basis set used in the present study was the $13s8p2d$ primitive Gaussian set given by Lie and Clementi [14]. This basis set was augmented with an f function with exponent 1.313 and contracted to $[6s4p2d1f]$. The CASSCF approach [15] was used in the first part of the calculations. The active space was chosen as the $2\sigma_g$, $2\sigma_u$, $3\sigma_g$, $1\pi_u$, $1\pi_g$, $3\sigma_u$ orbitals; the full distribution of 11 electrons into these orbitals gave 126 configuration state functions for the states of $^2\Pi_u$ symmetry. The calculations were performed in D_{2h} symmetry, however, $D_{\infty h}$ was maintained by imposing symmetry and equivalence restrictions on the wave functions. The calculations were concentrated on the $2\,^2\Pi_u$ and $3\,^2\Pi_u$ states although other states were also calculated at a limited number of internuclear distances. The full potential curve of the $2\,^2\Pi_u$ state was straightforward to calculate and single root excited state optimization was used. For the $3\,^2\Pi_u$ state the situation was complicated by crossings of other $^2\Pi_u$ states and at internuclear distances larger than 2.01 Å a root-averaged method was used.

The multireference configuration-interaction (MRCI) calculations [16] included all single and double excitations with respect to the CASSCF reference function; thus no reference configuration selection was used. CI benchmark calculations have shown that the CASSCF/MRCI approach is suitable for describing multiple bonds like the one in O_2^+ [17].

IV. RESULTS AND DISCUSSION

A. The overall He II excited spectrum

For reference, an overall He II excited spectrum was recorded in the present study and is shown in Fig. 1. A summary of the adiabatic and vertical ionization energies of the bands observed in this figure is given in Table I. The neutral ground-state electron configuration is

$$KK(2\sigma_g)^2(2\sigma_u)^2(3\sigma_g)^2(1\pi_u)^4(1\pi_g)^2 .$$

The He II excited outer-valence spectrum, seen in the energy range below 20 eV, includes transitions to the X, a, A, and b states. These states arise upon ionization from the three lowest molecular orbitals. This part of the spectrum is similar to the corresponding spectrum given in Ref. [1], however, the signal-to-noise ratio is considerably higher in the present spectrum. Therefore in some of the bands we observe more lines than previously. A detailed summary of the energies and relative intensities are planned to be presented in a separate publication [18]. It is interesting to note that the relative intensities in the vibrational progressions differ markedly compared to those in Ref. [1] obtained using He I radiation. This may reflect

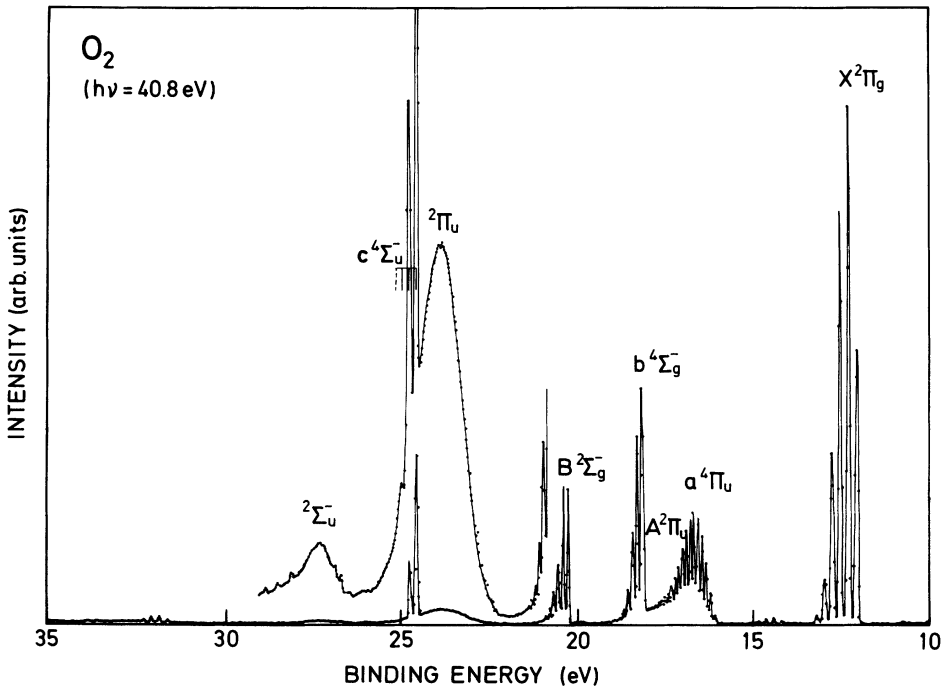

FIG. 1. A photoelectron spectrum of the O_2 molecule between 10 and 35 eV obtained by using monochromatic He IIα radiation at 40.8 eV. The resolution of the photoelectron lines was approximately 60 meV.

a variation in the electronic transition moment over the Franck-Condon region or the presence of other weak processes like autoionization.

B. Calculated potential curves and vibrational structure

Calculations were performed for the $2\,^2\Pi_u$ and $3\,^2\Pi_u$ states located at about 20 and 24 eV above the neutral ground state. The photoelectron band corresponding to the latter state is clearly seen in Fig. 1. The potential curves calculated for the $2\,^2\Pi_u$ and $3\,^2\Pi_u$ states are shown in Fig. 2. The Franck-Condon region for transitions from the neutral ground state is also indicated. The $2\,^2\Pi_u$ state is found to dissociate into an $O(^3P)+O^+(^2D^\circ)$ system, which has an energy of 22.06 eV as obtained by using atomic energies from Moore's tables [19] and a dissociation energy for the neutral molecule of 5.115 eV from Ref. [20]. As can be seen, the equilibrium bond distance is large as expected, from a comparison with the other two $^2\Pi_u$ states arising from the $(1\pi_u)^3(1\pi_g)^2$ configuration and also by a consideration of the orbital bonding properties.

Two more states of $^2\Pi_u$ symmetry can dissociate to the limit at 22.06 eV and according to the earlier calculations the $3\,^2\Pi_u$ state is one of these states [6–8]. This result was also obtained in the present study when the adiabatic potential curve was followed strictly. According to the calculations, there is a radical change in the wave function at the point of interaction between the potential curves occurring at 2.06 Å. At smaller internuclear dis-

TABLE I. Summary of the observed states of O_2^+ in Fig. 1. The vertical binding energies refer to the maximum intensity of the photoelectron band.

Electronic state	Adiabatic binding energy (eV)	Vertical binding energy (eV)
$X\,^2\Pi_g$	12.074	12.307
$a\,^4\Pi_u$	16.101[a]	16.703[a]
$A\,^2\Pi_u$	17.045[a,b]	17.643[a,b]
$b\,^4\Sigma_g^-$	18.171	18.171
$B\,^2\Sigma_g^-$	20.296	20.296
	20.35	20.35
$3\,^2\Pi_u$	21.32[c]	23.9
$c\,^4\Sigma_u^-$	24.564	24.564
$C\,^2\Sigma_u^-$		27.3

[a,b]From Refs. [1] and [4].
[c]Extrapolated value obtained from the observed and calculated vibrational structure.

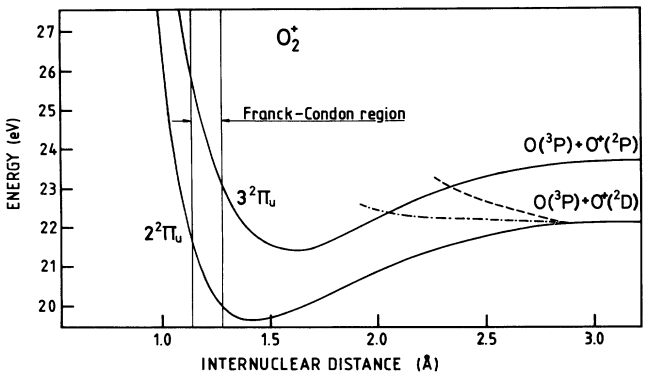

FIG. 2. Full lines: Potential curves obtained for the $2\,^2\Pi_u$ and $3\,^2\Pi_u$ states arising from the $1\pi_u^3 1\pi_g^2$ electron configuration. Dotted lines: Potential curves obtained for two many-electron states of $^2\Pi_u$ symmetry arising with leading configurations $(2\sigma_g)^2(2\sigma_u)^2(3\sigma_g)(1\pi_u)^4(1\pi_g)^1(3\sigma_u)$ (lower curve) and $(2\sigma_g)^2(2\sigma_u)^2(3\sigma_g)(1\pi_u)^4(3\sigma_u)^2$ (upper curve). The Franck-Condon region for transitions from the neutral ground state is also shown. The center of the Franck-Condon region is located at 1.207 52 Å.

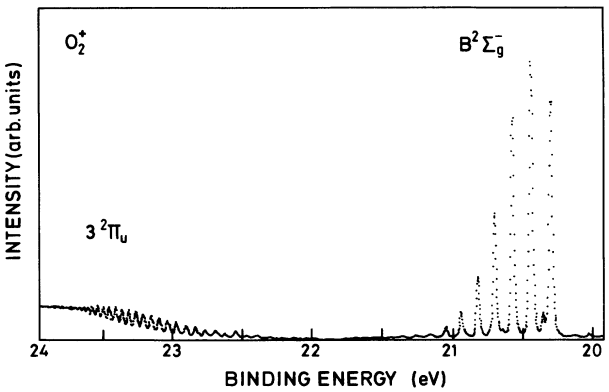

FIG. 3. A detail of the He II excited photoelectron spectrum of the O_2 molecule between 20 and 24 eV showing the lines associated with transitions to the $B\,^2\Sigma_g^-$ and $3\,^2\Pi_u$ states related to the $1\pi_u^3 1\pi_g^2$ electron configuration. The resolution was about 25 meV.

tances the state is determined essentially by the $(1\pi_u)^3(1\pi_g)^2$ whereas at larger distances than 2.06 Å it is described primarily by the many-electron configuration $(2\sigma_g)^2(2\sigma_u)^2(3\sigma_g)(1\pi_u)^4(1\pi_g)^1(3\sigma_u)$. The latter part of the potential curve is shown by a dash-dotted line in Fig. 2.

At an internuclear distance of about 2.12 Å the potential curve obtained for the $(1\pi_u)^3(1\pi_g)^2 3\,^2\Pi_u$ state is crossed by the curve of another repulsive many-electron state which gives rise to a new adiabatic pathway down to the dissociation limit at 22.06 eV. This interacting state has the leading configuration $(2\sigma_g)^2(2\sigma_u)^2(3\sigma_g)(1\pi_u)^4(3\sigma_u)^2$ and its potential curve is represented in Fig. 2 by a dashed line.

The curve that is obtained by following the $(1\pi_u)^3(1\pi_g)^2$ configuration does not go to a dissociation limit at 22.06 eV but to the next limit at 23.75 eV corresponding to a separated $O(^3P)+O^+(^2P)$ system. It is shown below that this curve corresponds very well to the experimental results, in particular the vibrational structure. The curve is represented by a full line in Fig. 2.

For both the $2\,^2\Pi_u$ and the $3\,^2\Pi_u$ states the vibrational energy levels and also Franck-Condon factors for the various vibrational levels were calculated and the results are summarized in Table II. The calculations were carried out using a method similar to that suggested in Ref. [21] using the calculated CI potential functions. The vibrational constants for the $2\,^2\Pi_u$ state were found to be $\omega_e = 0.106$ eV and $\omega_e x_e = -0.001\,06$ eV by fitting a second-degree polynomial to the calculated vibrational energy levels. The corresponding values for the $3\,^2\Pi_u$ state are $\omega_e = 0.107$ eV and $\omega_e x_e = -0.001\,14$ eV.

C. Experimental results for the energy range between 20 and 22 eV

Figure 3 shows a detail of the He II-excited spectrum in the region between 20 and 24 eV binding energy showing in the low-binding-energy part the vibrational progression related to the $B\,^2\Sigma_g^-$ ionic state and in the high-binding-energy part the band related to the $3\,^2\Pi_u$ ionic state. The latter will be discussed in the following section. In recordings with high statistics using monochromatic He IIα radiation, the B-state progression has been observed up to $v=9$. The latter of these vibrational components have relative intensities on the order of only 0.5% compared to the highest peak in the band and are possible to observe only due to the low background level. The energies and relative intensities are given in Table III.

By assuming a Morse potential for the $B\,^2\Sigma_g^-$ state and fitting a second-degree polynomial of the form

$$E = E_e + \omega_e(v+\tfrac{1}{2}) - \omega_e x_e (v+\tfrac{1}{2})^2$$

to the observed vibrational energies, where E_e represents the energy at the minimum of the potential curve, we obtain the following values for the vibrational constants: $\omega_e = 0.141$ eV and $\omega_e x_e = -0.0024$ eV. From these values the dissociation limit is found to be 22.29 eV. This corresponds well to the energy 22.06 eV that can be calculated for the separated $O(^3P)+O^+(^2D^\circ)$ system. The energy obtained from the Morse curve is slightly higher, which may suggest the presence of a low potential barrier towards dissociation. However, it is also possible that the vibrational levels converge more rapidly than predicted by the Morse curve close to the dissociation limit. It may be noticed that if the vibrational constants given in Ref. [20] are used, rather substantial deviations from the observed energies are obtained for the higher vibrational levels.

Figure 4 shows the spectrum of $B\,^2\Sigma_g^-$ state recorded at high resolution with He Iα radiation at 21.22 eV. In this study, neon was mixed with the oxygen gas in order to determine the photoelectron line shape and width. A detail of the Ne lines excited with the He Iβ component at 23.087 eV is inserted in the figure and as can be seen the linewidth was 5 meV. About 3.5 meV of this is due to Doppler broadening and hence the spectrometer

broadening is of similar size. As can also be seen from this spectrum, the photoelectron lines of neon are symmetric. The overall appearance of the band is similar to that shown in Fig. 3, however, due to the high resolution a significant asymmetrical broadening of the individual lines is readily seen. This is more clearly seen in Fig. 5 which shows a detail of the He I excited photoelectron spectrum of the O_2 molecule between 20.2 and 21.2 eV. As discussed below, this can be interpreted in terms of a partly resolved rotational structure.

It should be noted that the relative intensities of the vibrational lines in the He I excited spectrum of Fig. 4 differ markedly from those observed in the He II excited spectrum of Fig. 3. This may suggest that there is a dependence of the photoionization cross section on the photon energy which should be particularly pronounced in the He Iα spectrum where the kinetic energies are very low. If we assume that the relative intensities in the He II excited spectrum are independent of the electronic transition moment, a calculation of the Franck-Condon factors can be used to obtain the equilibrium bond distance of the $B\,^2\Sigma_g^-$ state. Using the simple harmonic approximation and the Ansbacher recursion formulas good agreement with the experimental relative intensities was obtained at a bond distance of 1.29(3) Å. This is in good agreement with the value 1.29(8) given in Ref. [10] where the figure in parentheses represents the third decimal which is uncertain.

Figure 6 shows the profile of the $v=0$ peak in the spectrum corresponding to the $B\,^2\Sigma_g^-$ state in greater detail. As can be seen, the line has a shoulder on the high-binding-energy side an a long tail of low intensity on the low-binding-energy side. The figure also shows a simulated rotational profile. This line shape was derived by a summation of 75 Gaussian lines, each representing the transition between well-defined rotational states of the initial and final states with $\Delta N=0$ or ± 2. The bond distance used for the initial state was 1.207 52 Å and for the final state 1.298 Å. In order to reproduce the experimental profile a much higher intensity had to be assumed for the $\Delta N=0$ transitions than for $\Delta N=\pm 2$. The relative intensities used were 1 and 0.27, respectively. The Gaussian lines were given a width of 4 meV [full width at half maximum (FWHM)], as would be expected from the

TABLE II. Vibrational energies and Franck-Condon factors obtained for the calculated potential curves shown in Fig. 2. The calculated adiabatic binding energies (E_B^{ad}), i.e., the energies of the 0−0 transitions, are given in eV.

	$2\,^2\Pi_u$ state		$3\,^2\Pi_u$ state	
Vibrational quantum number v	Vibrational energy (eV) $E_B^{ad}=19.69$	Franck-Condon factor	Vibrational energy (eV) $E_B^{ad}=21.49$	Franck-Condon factor
0	0.000	0.0011	0.000	0.720×10^{-9}
1	0.108	0.0056	0.094	0.169×10^{-7}
2	0.214	0.0150	0.192	0.132×10^{-6}
3	0.316	0.0285	0.294	0.770×10^{-6}
4	0.413	0.0421	0.392	0.316×10^{-5}
5	0.506	0.0548	0.487	0.996×10^{-5}
6	0.597	0.0674	0.578	0.261×10^{-4}
7	0.688	0.0772	0.666	0.601×10^{-4}
8	0.778	0.0828	0.752	0.126×10^{-3}
9	0.867	0.0836	0.836	0.240×10^{-3}
10	0.954	0.0807	0.919	0.429×10^{-3}
11	1.038	0.0749	1.000	0.716×10^{-3}
12	1.121	0.0674	1.080	0.113×10^{-2}
13	1.202	0.0590	1.158	0.168×10^{-2}
14			1.233	0.240×10^{-2}
15			1.307	0.328×10^{-2}
16			1.379	0.432×10^{-2}
17			1.449	0.549×10^{-2}
18			1.517	0.678×10^{-2}
19			1.582	0.815×10^{-2}
20			1.645	0.955×10^{-2}
21			1.706	0.109×10^{-1}
22			1.764	0.123×10^{-1}
23			1.820	0.134×10^{-1}
24			1.874	0.144×10^{-1}
25			1.924	0.151×10^{-1}
26			1.972	0.152×10^{-1}
27			2.016	0.143×10^{-1}
28			2.056	0.122×10^{-1}
29			2.091	0.909×10^{-2}

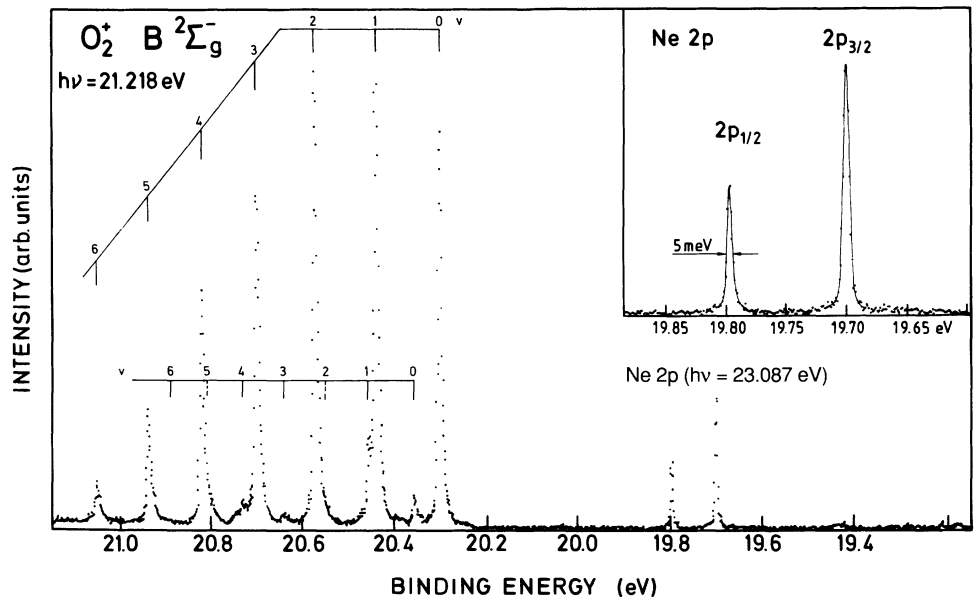

FIG. 4. A detail of the He I excited photoelectron spectrum of the O_2 molecule between 19.2 and 21.1 eV showing the lines associated with transitions to the $B\,^2\Sigma_g^-$ state. Inserted is a spectrum showing the Ne $2p$ lines excited by the He Iβ component at 23.087 eV. All lines in the figure were recorded simultaneously from a gas mixture of Ne and O_2. Thus the Ne lines show the true spectrometer line shape at the recording of the O_2 spectrum. The channel width was 1 meV.

combined effect of the Doppler and spectrometer broadenings, and the rotational levels from $N=0$ to 25 in the initial state were included for each ΔN. For the relative intensities of the components corresponding to a given value of ΔN the Boltzmann distribution was used and applied to the neutral molecule using a temperature of 293 K. Calculations using 90 Gaussians gave an almost identical result.

As can be seen from Fig. 6, the calculated line profile reproduces very well the experimental profile. The intensity in the experimental spectrum is higher than the calculated one in both the high- and low-energy tails of the

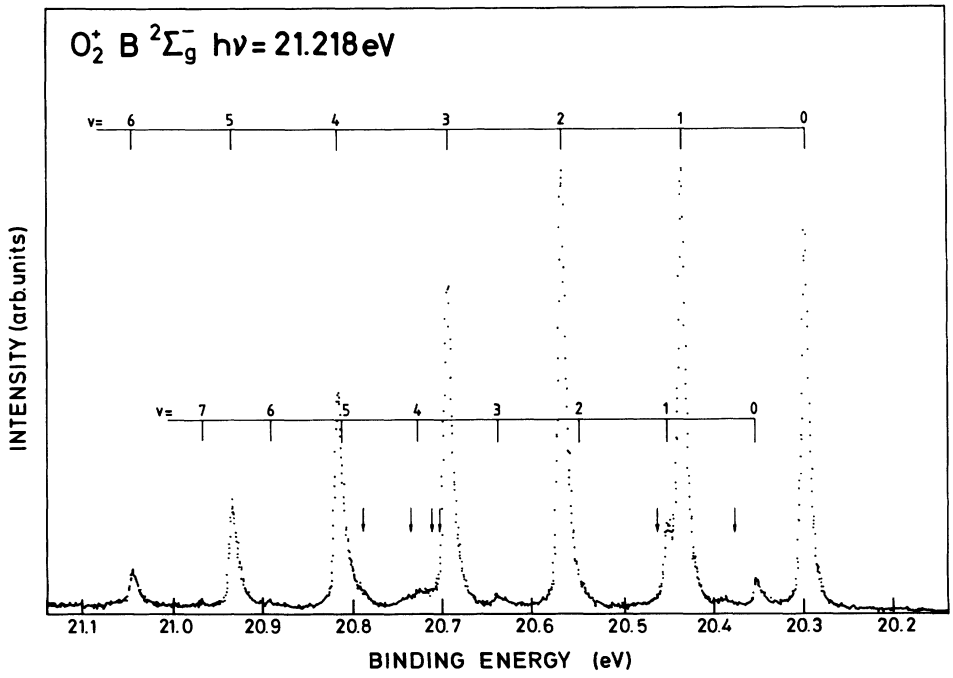

FIG. 5. A detail of the He I excited photoelectron spectrum of the O_2 molecule between 20.2 and 21.1 eV showing the spectrum of Fig. 4 on an enlarged energy scale. A number of weak lines are observed which seem to form a vibrational progression ($v=0-7$) that starts at 20.35 eV. The arrows indicate the positions where contributions from autoionization of atomic oxygen are expected. The channel width was 0.5 meV.

TABLE III. Vibrational energy levels for the $B\,^2\Sigma_g^-$ state of O_2^+ and relative intensities in transitions from the neutral ground state.

Vibrational quantum number v	Binding energy (eV)	Relative intensity
0	20.296	0.84
1	20.433	1.00
2	20.563	0.70
3	20.690	0.38
4	20.812	0.18
5	20.928	0.079
6	21.040	0.034
7	21.146	0.015
8	21.249	0.008
9	21.348	0.005

line, which is probably mainly due to the presence of higher rotational components, not included in the calculations. The line profile is very sensitive to the parameter values, and the set of data used is the one giving the best fit with the restriction that the intensities for the $\Delta N=+2$ and -2 transitions be held equal. The edge of the shoulder on the high-binding-energy side of the line corresponds to the band head for the $\Delta N=2$ transition, that is, the S branch. The head is formed at a position corresponding to $J=14$ in the initial state. The edge on the high-binding-energy side of the most intense part corresponds to the band head of the $\Delta N=0$ transition. In this case no reversal of the rotational transition energies occurs. The $\Delta N=-2$ transitions are reflected primarily in the long tail on the low-binding-energy side of the line.

It may be noticed finally that while the Franck-Condon analysis gives the change in bond distance from the neutral ground state but not the sign, the rotational analysis proves that the bond distance is larger in the final state. It is noteworthy also that this fit gives a value of the bond distance which is in close agreement with the value quoted in Ref. [20].

In addition to the strong progression associated with the $B\,^2\Sigma_g^-$ cationic state, a number of weaker lines can be clearly seen in both the He I and He II excited spectra (cf. Figs. 3–5). Since the lines have the same relative intensities in all spectra, independent of gas pressure and excitation energy, and cannot be identified as arising from any impurity in the sample gas, we assume that they correspond to an ionic state of the oxygen molecule. The energies and relative intensities are given in Table IV. As indicated in Fig. 5, the lines seem to form a progression with successively decreasing spacings towards higher binding energy. One reason for carrying out the calculations was therefore to see if an assignment to the $2\,^2\Pi_u$ state would be justified by the calculated results. As can be seen from Table II the lines are indeed observed in the correct energy region. There is also a good agreement between the observed energies and calculated vibrational levels, however, only assuming that the observed lines correspond to rather high vibrational quantum numbers. Thus such an assignment would imply that a number of lines corresponding to low vibrational levels would be unobserved in the experimental spectrum which seems

TABLE IV. Weak structures associated with vibrational excitations in the 20–21-eV energy region. The last figure in the binding energy is uncertain. The approximate values correspond to estimated energies for unresolved lines (compare Figs. 4 and 5).

Vibrational quantum number v	Binding energy (eV)	Vibrational energy spacing (meV)
0	20.351	0
1	20.450	99
2	≈20.544	≈94
3	20.637	≈93
4	20.726	89
5	≈20.810	≈84
6	20.890	≈80
7	20.968	78

unreasonable. The interpretation of this progression will therefore have to await further experimental and theoretical studies.

By fitting a second-degree polynomial to the energies of the observed lines, and assuming that these lines represent a vibrational progression, we obtain the following values for the vibrational constants of the state: $\omega_e=0.103$ eV and $\omega_e x_e=-0.0018$ eV. From these values a Morse potential curve can be estimated with a dissociation limit of 21.76 eV. A high accuracy cannot be expected since only rather few, weak, and partly unresolved vibrational lines are observed. However, this value corresponds well to the expected energy 22.06 eV of the $O(^3P)+O^+(^2D^\circ)$ state of the separated molecular ion as obtained from Refs. [19,20]. Hence the dissociation limit appears to be the same as for the $B\,^2\Sigma_g^-$ state.

The relative intensities between the peaks are not easy to determined accurately due to the weakness of the lines and overlap with peaks of the $B\,^2\Sigma_g^-$ state. However, the $v=0$ and 3 components are well resolved and have an in-

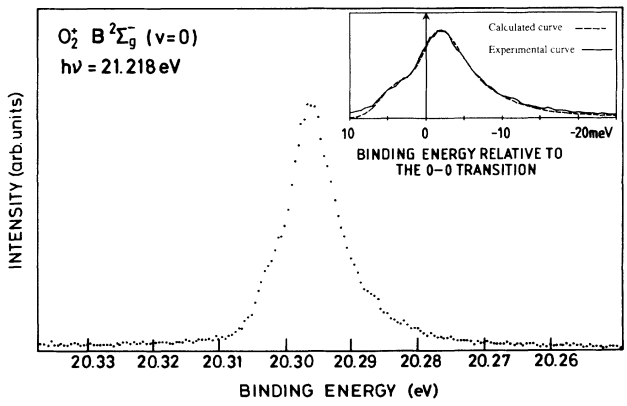

FIG. 6. The $v=0$ vibrational component of the $B\,^2\Sigma_g^-$ state. The inserted figure shows the same line along with a simulated line profile obtained by adding rotational transitions broadened by a Gaussian with a width of 4 meV. The $N=0$–25 levels were included and the $\Delta N=0,\pm2$ transitions were considered. The weights for $\Delta N=0,\pm2$ used in this simulation were 1 and 0.27, respectively.

tensity ratio of 1:0.38. A calculation of the Franck-Condon factors using the harmonic approximation shows that this ratio corresponds to an equilibrium bond distance of 1.29 Å for the ionic state, that is, the bond distance obtained in this manner is approximately the same as for the $B\,^2\Sigma_g^-$ state.

Additional weak structures can be seen in Fig. 5. Particularly apparent are those at 20.38, 20.71, 20.74, and 20.79 eV. These structures can be associated with autoionization in neutral oxygen atoms produced via dissociation of neutral or singly ionized molecules. The energies where such contributions may occur in the spectrum can be obtained from the atomic data of Ref. [19] and are indicated in Fig. 5 by the arrows. The transitions have been studied previously by means of Penning ionization electron spectroscopy [22] using metastable helium atoms with energies of 20.61 and 19.81 eV and by synchrotron-radiation photoelectron spectroscopy [23] in the energy range between 19 and 22 eV. In this range a strong production of O^+ ions has been observed [24] in a study of photoionization and photodissociation processes of O_2. However, the autoionization lines can also be very clearly observed in the He II excited spectrum [25] and the intensity observed in the present spectrum may thus at least in part be due to the He II component in the radiation from the uv source.

D. Experimental results for the energy range between 22 and 26 eV

Figure 7 shows the overall spectrum of the energy region between 22 and 26 eV. It displays two dominating features, one broad band (seen also in Fig. 2) centered at 23.9 eV and two very narrow lines between 24.5 and 25 eV. The former band is associated with transitions to the $3\,^2\Pi_u$ state derived from the $1\pi_u^3 1\pi_g^2$ ionic-state electron configuration. The intensity is comparatively high (cf. Fig. 1) as has been predicted theoretically. The band has in earlier studies been considered structureless [1,2]. However, as can be seen from Fig. 7 it contains a very long vibrational progression extending over the first part of the band. Figure 8 shows this part of the spectrum recorded with high resolution. In Table V the energies are given.

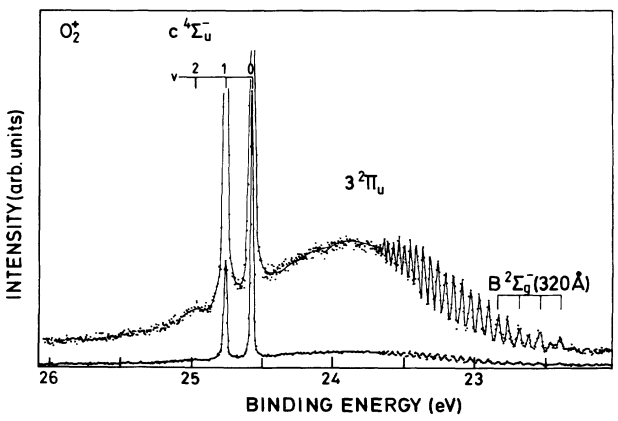

FIG. 7. A detail of the He II excited photoelectron spectrum of the O_2 molecule between 22 and 26 eV showing the lines associated with transitions to the $3\,^2\Pi_u$ and $c\,^4\Sigma_u^-$ states.

The spacings are on the order of 80 meV in the beginning of the band, and decrease gradually towards the end of the progression. The convergence limit is approximately 23.83 eV. Overlapping features are seen in the beginning of the band due to transitions to the $B\,^2\Sigma_g^-$ state induced by the 320-Å component in the radiation from the uv source. The strongest lines of this progression are indicated in the inset of Fig. 8. However, at least one vibrational component belonging to the $3\,^2\Pi_u$ state can be seen at lower energy. The first clearly observed line present in all spectra is seen at a binding energy of 22.30 eV. This line is quite broad and possibly consists of more than one component.

As seen from the calculated results, the line at 22.30 eV cannot be the lowest vibrational component. In order to assign the vibrational peaks we have therefore compared the energy spacings between the experimental and calculated data. This can be done since the calculated potential curves are expected to be accurate. The best fit is obtained if the line at 22.30 eV is associated with the $v=10$ vibrational level or possibly the $v=11$ level. Assuming that the first line in the spectrum is $v=10$, we have obtained the following values for the vibrational constants

TABLE V. Vibrational energies and spacings of the inner-valence photoelectron band associated with transitions to the $3\,^2\Pi_u$ state in the 22–24-eV range.

Line number	Vibrational quantum number[a]	Energy (eV)	Vibrational spacing (meV)
1	10	22.300	
2	11	22.393	93
3	12	22.461	68
4	13	22.538	76
5	14	22.616	79
6	15	22.684	67
7	16	22.763	80
8	17	22.833	70
9	18	22.900	67
10	19	22.965	65
11	20	23.029	64
12	21	23.091	63
13	22	23.148	57
14	23	23.205	57
15	24	23.257	52
16	25	23.309	52
17	26	23.361	52
18	27	23.408	47
19	28	23.452	44
20	29	23.494	42
21	30	23.534	40
22	31	23.572	37
23	32	23.602	31
24	33	23.638	36
25	34	23.664	25
26	35	23.689	25
27	36	23.708	19
28	37	23.732	24

[a]The numbering has been obtained from a comparison with the calculated energy levels and is tentative (see text).

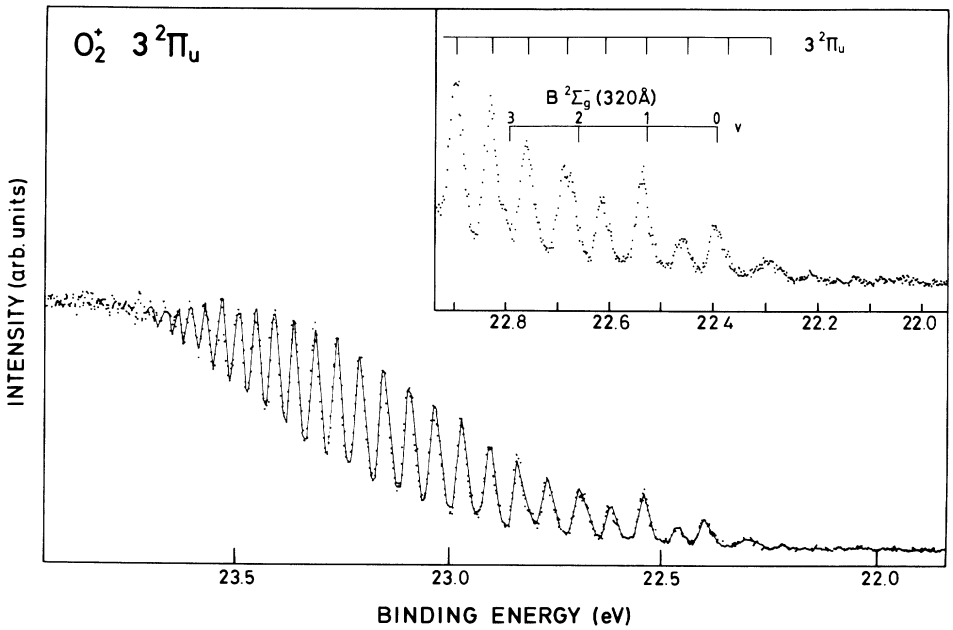

FIG. 8. A detail of the He II excited photoelectron spectrum of the O_2 molecule between 22.0 and 24 eV showing the lines associated with transitions to the $3\,^2\Pi_u$ state. On the low-binding-energy side weak lines are seen which correspond to transitions to the $B\,^2\Sigma_g^-$ state. They were induced by the 320-Å line in the He radiation and are seen more clearly in the inset figure.

of the $3\,^2\Pi_u$ state by fitting a second-degree polynomial to the observed energies: $\omega_e = 0.110$ eV and $\omega_e x_e = -0.001\,19$ eV. However, since the anharmonicity constant is small these values change only slightly if other vibrational assignments are made. These values are in close agreement with the corresponding calculated data (cf. above). From these energies an adiabatic binding energy of 21.321 eV is obtained. As indicated above, the dissociation limit is found to be 23.83 eV, which corresponds well to the energy 23.75 eV of the $O(^3P)+O^+(^2P)$ state of the separated molecular ion as obtained from Refs. [19,20].

The repulsive potential curves calculated for the two many-electron states of $^2\Pi_u$ symmetry cross the potential curve of the $3\,^2\Pi_u$ state at 22.4 and 23.0 eV. At these energies strong local interactions between the states should be reflected by irregularities in the vibrational structure. In particular, the adiabatic potential curves would predict a cutoff of the vibrational structure at 22.4 eV or at least strong perturbations above this energy. This is clearly not the case, except possibly for the seemingly large width of the peak at 22.30 eV. However, since the intensity of this peak is very low and weak lines of other origins could be present, it must be concluded that interactions with the repulsive states are not clearly reflected by the present spectra. Thus, at the present level of resolution, the spectrum is apparently well described by the potential curve associated with the $1\pi_u^3 1\pi_g^2$ electron configuration.

On the high-binding-energy side of the band associated with the $3\,^2\Pi_u$ state, two sharp lines are observed which reflect the transitions to the $v=0$ and 1 levels of the $c\,^4\Sigma_u^-$ state (cf. Fig. 7). In addition, a very weak feature at higher binding energies indicates the position of the $v=2$ level. Our identification of the lines agrees with that made in Ref. [1], however, the energy of the $v=0$ state is lower. According to Gilmore [26] the adiabatic energy of this state is 24.56 eV, which is very close to the helium $1s_{1/2}$ lines at 24.587 eV. In Ref. [1] a value of 24.577 eV was given, which may be obtained if the overlap between the lines is not considered and the admixture of helium gas in the sample cell is large. In the present investigation we have therefore carried out separate studies in the energy region of the $c\,^4\Sigma_u^-$ state under conditions giving very little helium in the gas cell. Furthermore, when He IIα excitation was used the radiation was monochromatized in order to remove other radiation components. In addition to the He IIα excitation at 40.814 eV, also He IIβ excitation at 48.372 eV was used. A spectrum obtained with the latter radiation is shown in Fig. 9. Due to the overlapping structures from the a and A states excited by the He IIα line, which was not completely removed by the monochromator, it is not possible to obtain a very accurate value of the relative intensity between the $v=1$ and 0 lines. The adiabatic binding energy obtained from these studies is 24.564 eV (cf. Table VI) in close agreement with Ref. [26].

By carrying out a Franck-Condon analysis of the vibra-

TABLE VI. Vibrational energy levels in the 24–25-eV energy region associated with the $c\,^4\Sigma_u^-$ state of O_2^+.

Vibrational quantum number v	Binding energy (eV)	Relative intensity (FWHM)
0	24.564	1
1	24.756	0.42
2	25.005	0.015

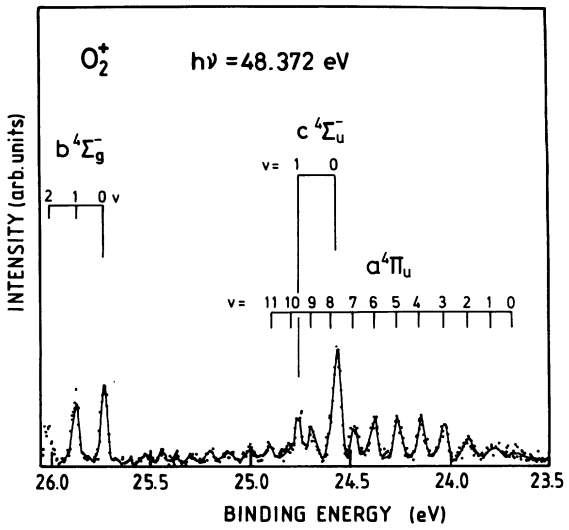

FIG. 9. A detail of the He II excited photoelectron spectrum of the O_2 molecule showing the $c\,^4\Sigma_u^-$ state excited with the He IIβ component and the $a\,^4\Pi_u$ and $b\,^4\Sigma_g^-$ states excited by the He IIα radiation. The binding-energy scale refers to the $c\,^4\Sigma_u^-$ state.

tional lines in Figs. 7 and 9, using the harmonic approximation and an intensity ratio between the lines of 0.42:1, the equilibrium bond distance of the $c\,^4\Sigma_u^-$ state is found to be 1.16 Å, using a bond distance of 1.207 52 Å for the neutral ground state. This is close to the value 1.162 Å given in Ref. [20].

The intensity at the maximum of the $v=2$ line is much too low to fit into an ordinary Franck-Condon intensity distribution. However, as can be seen from the enhanced spectrum of Fig. 7, the $v=2$ line is about four times as broad as the other two lines, so a proper comparison of the relative intensities would involve the peak areas. When this is done the intensity is found to be about 1.5% of the $v=0$ line, while the expected intensity according to a Franck-Condon distribution would be about 8%. This implies that the intensity is still too small by almost an order of magnitude. Therefore it is most likely that the electronic state is strongly predissociated due to a curve crossing occurring in this energy range and that the interacting state gives rise to such a distortion of the c-state potential curve that a large part of the transitions in the $v=2$ range tend to go to the dissociation continuum. This agrees with the large width of 40 meV of the $v=2$ line, while it is only 10 meV for the $v=0$ component. This corresponds to a lifetime on the order of only 2×10^{-14} s for the $v=2$ level. Even the $v=1$ line is slightly broadened compared to the $v=0$ line, which suggests that also this level is influenced by the interaction with the dissociation continuum (e.g., [6]).

V. CONCLUSIONS

A high-resolution study of the inner-valence region of the O_2 photoelectron spectrum between 20 and 26 eV has been carried out. Vibrational structure has been observed in most photoelectron bands and the vibrational constants ω_e and $\omega_e x_e$ have been derived as well as dissociation energies. CI calculations have been performed for the states of $^2\Pi_u$ symmetry in the region between 20 and 26 eV. The calculated potential curve of the $3\,^2\Pi_u$ state is in good agreement with the experimental results. A hitherto unobserved vibrational progression in the $3\,^2\Pi_u$ state associated with a leading $1\pi_u^3 1\pi_g^2$ electron configuration shows that the dissociation limit for this state is 23.75 eV. This corresponds to a separation into an $O(^3P)+O^+(^2P)$ system and not $O(^3P)+O^+(^2D)$ with a dissociation limit at 22.06 eV as obtained from the adiabatic potential curves. A pronounced rotational profile is observed for the vibrational lines associated with the $B\,^2\Sigma_g^-$ state slightly above 20 eV binding energy. A rotational analysis has been made which shows that the $\Delta N=0,\pm2$ transitions occur with an intensity ratio of 1:0.27. The bond distance obtained from this analysis is in good agreement with the value 1.298 Å derived earlier [20]. A weak vibrational progression in the range of the $B\,^2\Sigma_g^-$ state observed in both He I and He II excited spectra indicates the presence of another bound electronic state in this energy region. At the present level of statistics and resolution it is not possible to make a conclusive assignment of this progression. Some evidence, like the binding-energy range, the bond distance obtained from the relative intensities, the dissociation limit, and comparison to the results of Refs. [3,4,6], indicate that it might correspond to the lowest $^2\Delta_g$ state. However, improved studies are currently being carried out and the results of these are planned to be published later.

[1] O. Edqvist, E. Lindholm, L. E. Selin, and L. Åsbrink, Phys. Scr. **1**, 25 (1970).
[2] J. L. Gardner and J. A. R. Samson, J. Chem. Phys. **62**, 4460 (1975).
[3] N. Jonathan, A. Morris, M. Okuda, K. J. Ross, and D. J. Smith, J. Chem. Soc. Faraday Trans. II **70**, 1810 (1974).
[4] H. van Lonkhuyzen and C. A. de Lange, J. Electron Spectrosc. **27**, 255 (1982).
[5] P. Baltzer, M. Carlsson-Göthe, B. Wannberg, and L. Karlsson, Rev. Sci. Instrum. **62**, 630 (1991).
[6] N. H. F. Beebe, E. W. Thulstrup, and A. Andersen, J. Chem. Phys. B **64**, 2080 (1976).
[7] N. Honjou, K. Tanaka, K. Ohno, and H. Taketa, Mol. Phys. **35**, 1569 (1978).
[8] C. M. Marian, R. Marian, S. D. Peyerimhoff, B. A. Hess, R. J. Buenker, and G. Seger, Mol. Phys. **46**, 779 (1982).
[9] R. N. Dixon and S. E. Hull, Chem. Phys. Lett. **3**, 367 (1969).
[10] Peter Baltzer, Björn Wannberg, and Mats Carlsson Göthe, Rev. Sci. Instrum. **62**, 643 (1991).
[11] P. Baltzer, B. Wannberg, and L. Karlsson (unpublished).
[12] P. Baltzer and L. Karlsson (unpublished).
[13] P. Baltzer and L. Karlsson, Phys. Rev. A **38**, 2322 (1988).
[14] G. C. Lie and E. Clementi, J. Chem. Phys. **60**, 1275 (1974).
[15] P. E. M. Siegbahn, J. Almlöf, A. Heiberg, and B. O. Roos, J. Chem. Phys. **74**, 2384 (1981).

[16] P. E. M. Siegbahn, Int. J. Quantum Chem. **23**, 1869 (1983).
[17] C. W. Bauschlicher and S. R. Langhoff, J. Chem. Phys. **86**, 5595 (1987).
[18] P. Baltzer, B. Wannberg, and L. Karlsson (unpublished).
[19] C. E. Moore, *Atomic Energy Levels,* Natl. Bur. Stand. (U.S.) Circ. No. 467 (U.S. GPO, Washington, DC, 1949).
[20] K. P. Huber and G. Herzberg, *Molecular Spectra and Molecular Structure IV. Constants of Diatomic Molecules* (Van Nostrand Reinhold, New York, 1979).
[21] W. R. Jarmain, J. Quant. Spectrosc. Radiat. Transfer **11**, 421 (1971).
[22] V. Cermák and J. Srámek, J. Electron Spectrosc. **2**, 97 (1973); V. Cermák, *ibid.* **6**, 135 (1975).
[23] A. A. Cafolla, T. Reddish, and J. Comer, J. Phys. B **22**, L273 (1989).
[24] L. E. Berg, P. Erman, E. Källne, S. Sorensen, and G. Sundström, Phys. Scr. (to be published).
[25] P Baltzer, B. Wannberg, and L. Karlsson (unpublished).
[26] F. R. Gilmore, The Rand Corp. Mem. RM-4034-PR, 1964 (unpublished).